Photoresponse properties of Au/(CoFe2O4-PVP)/n-Si/Au (MPS) diode

A. Buyukbas Ulusan
Gazi University
Adem Tataroglu (ademt@gazi.edu.tr)
Gazi University
S. altindal
Gazi University
Y. Azizian-Kalandaragh
Gazi University

Research Article

Keywords: (CoFe2O4-PVP) film, MPS diode, Photoresponse properties, Responsivity and sensitivity

Posted Date: February 23rd, 2021

DOI: https://doi.org/10.21203/rs.3.rs-248560/v1

Photoresponse properties of Au/($CoFe_2O_4$-PVP)/n-Si/Au (MPS) diode

A. Buyukbas Ulusan[1], A. Tataroglu[1], Ş. Altındal[1], Y. Azizian-Kalandaragh[2,3,4]

[1] Physics Department, Faculty of Sciences, Gazi University, Ankara, Turkey
[2] Department of Physics, University of Mohaghegh Ardabili, P.O. Box.179, Ardabil, Iran
[3] Engineering Sciences Department, Sabalan University of Advanced Technologies, Namin, Iran
[4] Photonics Research and Application Center, Gazi University, Ankara, Turkey

Corresponding author: ademt@gazi.edu.tr (A. Tataroglu)

Abstract

Photo-response properties of the Au/($CoFe_2O_4$-PVP)/n-Si (MPS) diode were investigated using current-voltage (I-V) measurements achieved under dark and various illumination conditions. The experimental results showed that the MPS diode has a good response to the illumination. Especially, in reverse-bias region, photocurrent (I_{ph}) increases with increasing illumination intensity (P) due to the formation of electron–hole pairs. The double-logarithmic I_{ph}-P plot has a good relation with 1.27 slope and such high value of slope indicates a lower density of the unoccupied trap level. This indicates that the diode exhibits a good photoconductive and photovoltaic behavior. The photo-to-dark current ratio confirms the photo-sensitivity of the diode. Thermionic emission (TE) theory was used to determine the diode electronic parameters such as saturation current (I_0), ideality factor (n) and barrier height (Φ_{B0}) and their values were calculated from the measured I-V data. Moreover, the Φ_{B0} and series resistance (R_s) were extracted from an alternative method suggested by Norde. All these parameters (Φ_{B0}, n, R_s, and I_0) decrease with increasing illumination intensity and there is a good linear correlation between Φ_{B0} and n as Φ_{B0} (n)=4.72x10^{-2}n+0.5464 eV. As a results, the fabricated MPS diode due to the excellent photo-response can be used for photovoltaic applications.

Keywords: *($CoFe_2O_4$-PVP) film;* MPS diode*; Photoresponse properties; Responsivity and sensitivity,*

1. Introduction

A metal-polymer-semiconductor (MPS) structures are formed by sandwiching organic polymers between M and S and they are similar to the metal-insulator-semiconductor (MIS) type Schottky-barrier diodes (SBDs) due to the dielectric property of the polymers. In recent years, organic polymers are often used in various electronic and optoelectronic device applications including photodiodes, solar cells, transistors, sensors, detectors, polymer integrated circuits [1-5]. When a diode is exposed to illumination, the electron-hole pairs are generated in near the depletion region of the diode. Then, these pairs are separated under applied electric field. On the other hand, this separation is more effective at in the reverse bias. The number of photo-generated charge carriers increases under illumination. Especially, in the

reverse bias region, these carriers create an additional current to the dark current. The reverse bias current is called as photocurrent (I_{ph}) and it determined by the amount of photo-generated charge carriers increases with illumination intensity [6,7]. Moreover, the increase number of charge carriers leads to an increase in photoconductivity. In addition, the responsivity is used for the evaluation of the performance of light sensitive devices such as photodiodes, phototransistors, and photovoltaic cells.

Today, the main technical and scientific problems are relevant to the increase in the of photo-current and decrease cost of the photodiode or solar cells and it is remaining a challenge problem to the researchers yet. When these devices are exposed to the illuminated, some of the electrons may be generated and they could be trapped or release from the trap. These trapping and releasing processes can be considered as charging and discharging respectively. Although sunlight contains a huge amount of energy, these devices are very inefficient to absorb these photons/energy and can only utilize a small portion of these photons because of many photons have not enough energy to form electron-hole pairs so they will simply pass straight through the device without affecting it. Therefore, in the last years, researchers have been focused on the developing new technologies that allows us to capture and convert this energy from the sun to provide electricity.

Most common polymers are polyvinyl-pyrrolidone (PVP), polyvinyl alcohol (PVA), polyvinyl acetate (PVAc), polyaniline (PANI) and polypyrrole (PPy). Among them, PVP and PVA have similar functional group as they are physically cross-linked. While PVP is an amorphous polymer, PVA is a semi-crystalline polymer. PVP and PVA are also water-soluble synthetic polymers [8-10]. Polymers have unique physical and chemical properties such as excellent film forming characteristics, high ionic conductivity, high absorption coefficient, moderate electrical conductivity, easy processibility, good thermal and mechanical stability, non-toxic and low cost [10-14]. Polymer thin films can be deposited using various techniques including electrospinning, sol-gel, drop/spin/dip-coating, and spray/ink- printing [15,16].

In our previous study, the electrical properties of MPS and MS diodes with and without the $CoFe_2O_4$-PVP interfacial layer have been compared [17]. In this study, photoresponse and electrical properties of the Au/($CoFe_2O_4$-PVP)/n-Si (MPS) diode were investigated under dark and different illumination intensities using the forward and reverse bias I-V measurements at

room temperature. Experimental results showed that the prepared Au/($CoFe_2O_4$-PVP)/n-Si (MPS) structure has a good response to the illumination.

2. Experimental details

Au/($CoFe_2O_4$-PVP)/n-Si (MPS) type structures were fabricated with deposited of ($CoFe_2O_4$-PVP) polymer interface layer on n-Si substrate. A detail information both on the chemical cleaning processes and formation on the grown of ($CoFe_2O_4$-PVP) polymer interlayer at Au/n-Si wafer can be found in our previous study [17]. The forward-reverse bias I-V measurements were carried out by using a voltage-current source (Keithley 2400) both in dark and under illumination range of 30-100 mW/cm^2 in the VPF-475 cryostat with four optical window. The fabricated MPS diode was illuminated with Newport/Oriel solar simulator and illumination level was determined by the ILT1700 research radiometer.

3. Results and Discussion

Both in dark and various illumination intensities, the I-V characteristics of the prepared Au/($CoFe_2O_4$-PVP)/n-Si (MPS) diode was analyzed with the help of the standard thermionic emission (TE) theory. To extract important diode parameters such as such as reverse saturation current (I_0), ideality factor (n) and barrier height (Φ_{B0}), and series-resistance (R_s) both TE and Norde-function were used. In the based on TE theory ($V \geq 3kT/q$), the current in the forward bias is given by [18,19],

$$I = I_0 \left[\left(\exp\left(\frac{q(V - IR_s)}{nkT} \right) - 1 \right) \right] \quad (1)$$

For a diode with series resistance (R_s), the V-IR_s term describes the voltage drop across R_s. The I_0 and n parameters can be extracted from the intercept and slope of the linear region of the forward-bias ln(I)-V plot for each temperature and illumination intensity, respectively. The I_0 and n are defined in the following equations,

$$I_0 = AA^*T^2 \exp\left(-\frac{q\phi_{B0}}{kT} \right) \qquad \text{and} \qquad n = \frac{q}{kT} \left(\frac{dV}{d(\ln I)} \right) \quad (2)$$

where, A is the diode area, A^* is the Richardson constant (=112 A/cm^2.K^2 for p-Si), and Φ_{B0} is the zero-bias barrier height and it can be calculated by using he experimentally obtained value of I_0 and Schottky/rectifier contact are (A). But, the main electrical parameters obtained from

the TE theory are usually deviated from the ideal case due to the existence of interfacial layer, R_s, barrier-inhomogeneity, and surface-states/traps.

Fig. 1 demonstrates the reverse and forward bias semi-logarithmic I-V characteristics of the MPS diode measured in dark and under illumination. The MPS diode exhibits a clear rectifying behavior in the dark. As seen in Fig. 1, the current under illumination is higher than the dark current, and the photocurrent increases with increasing illumination intensity. This behavior confirms that the MPS diode exhibits a good photoconductivity. Moreover, the change in the reverse-bias current is much greater than the change in the forward-bias current. Photocurrent is significant in reverse-bias region because of in this region both the inner and external electric field has some direction and hence total electric field becomes strong when compared forward bias region. Under this high-electric field the recombination of the electrons and holes at the junction become decrease. As can be clearly seen in Fig. 1, the transient I_{ph} increases with increasing illumination level. In the other words, the increase in reverse current is the result of generated electron-hole pairs under illumination effected and called as photocurrent.

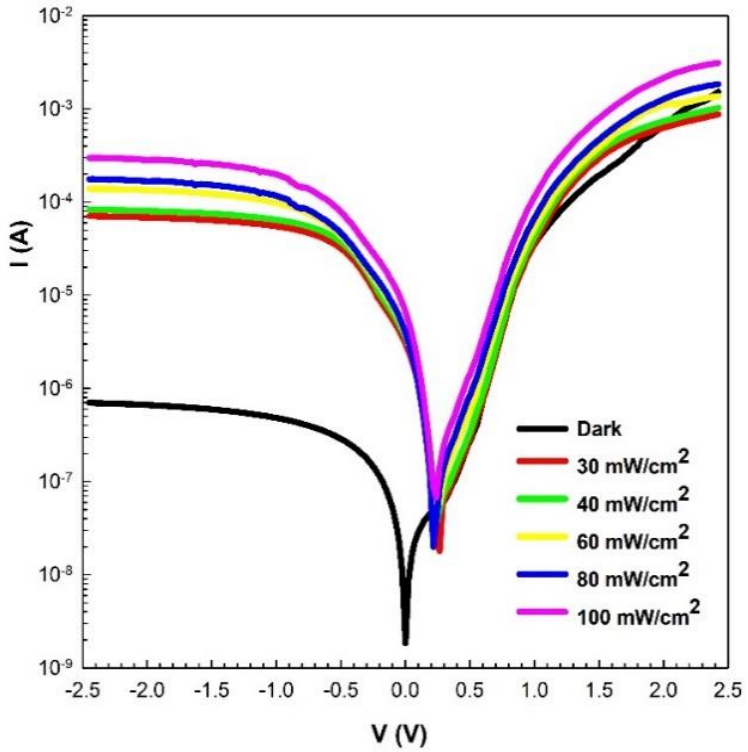

Fig. 1. Semi-logarithmic I-V characteristics of the MPS diode.

When a diode is illuminated, the current carriers (electrons and holes) are generated in depletion region where the carrier concentration is lower than its equilibrium. The current generated by illumination adds to the dark current. Thus, the current known as photocurrent is larger than the dark current. The photocurrent is proportional to illumination intensity [20-24]. Since electrons absorb enough energy by photons rather than the forbidden bandgap (E_g) of the semiconductor, then many electrons in the valence band (E_v) can be jumped into the conduction band (E_c) or trap to trap.

The diode electronic parameters including I_0, n and Φ_{B0} obtained from the forward-bias I-V characteristics under dark and different illumination conditions, are shown in Table 1. It is seen that these parameters depend on the intensity of illumination. The n and Φ_{B0} value decrease with increasing illumination intensity. Besides, the n value was found to be much greater than 1. This result results from the presence of interfacial layer and surface states, image-force lowering, and series resistance [25-29].

Table 1. Diode electronic parameters obtained from the various methods.

P (mW/cm^2)	**I_0 (A) (TE)**	**n (TE)**	**Φ_{B0} (eV) (TE)**	**Φ_B (eV) (Norde)**	**R_s (kΩ) (Norde)**	**R_{sh} (MΩ) (Ohm)**	**R_s (kΩ) (Ohm)**
0 (Dark)	4.920×10^{-9}	5.122	0.787	0.836	1.180	3.4886	1.530
30	5.843×10^{-9}	4.988	0.782	0.831	0.903	0.0346	2.730
40	7.259×10^{-9}	4.901	0.777	0.827	0.880	0.0296	2.330
60	9.433×10^{-8}	4.710	0.770	0.821	0.714	0.0176	1.750
80	1.230×10^{-8}	4.570	0.763	0.818	0.616	0.0139	1.360
100	1.588×10^{-8}	4.493	0.757	0.813	0.434	0.0082	0.803

As can be seen in Table 1 and Fig. 2, there is a good linear correlation between Φ_{B0} and n as $\Phi_{B0}(n)=4.72\times10^{-2}n+0.5464$ eV and hence the value of Φ_{B0} was found as 0.5936 eV for n=1 (ideal case). The obtained higher values of n can be attributed to the existence of ($CoFe_2O_4$-PVP) organic interlayer, its thickness, barrier inhomogeneity at Au/n-Si surface, surface states/traps, and dislocations.

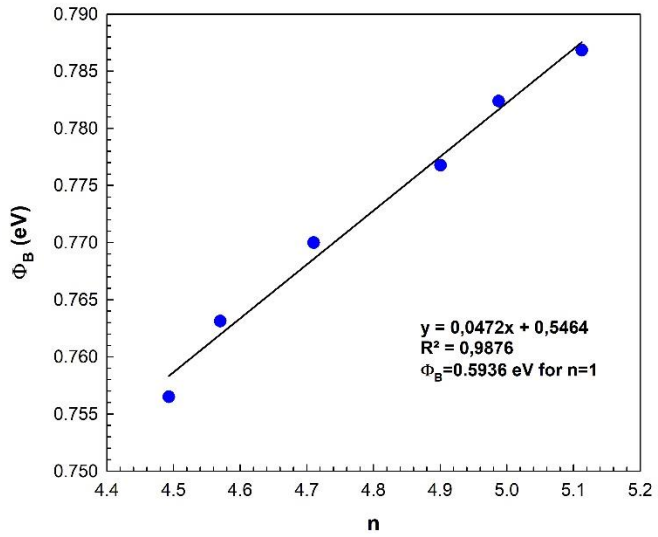

Fig. 2. The plot of Φ_{B0}-n characteristics.

In addition, Norde proposed an alternative method to extract barrier height (Φ_B) and series resistance (R_s) [30]. According to this method, F(V) is defined as Norde function and is given by,

$$F(V) = \frac{V}{\gamma} - \frac{kT}{q}\left[\ln\left(\frac{I(V)}{AA^*T^2}\right)\right] \tag{3}$$

where γ is an integer (dimensionless) greater than the obtained n value for the MPS diode. The Φ_B value is calculated from the value corresponding to the minimum of the F(V)-V plot and is given as follows,

$$\Phi_B = F(V_{min}) + \frac{V_{min}}{\gamma} - \frac{kT}{q} \tag{4}$$

the R_s value is calculated as follows:

$$R_s = \frac{kT(\gamma - n)}{qI_{min}} \tag{5}$$

where I_{min} is the current value corresponding to the V_{min} value. Fig. 3 shows the Norde function F(V) versus V plots for MPS diode. It is clear that the F(V)-V plots show minimum. The calculated Φ_B and R_s values are given in Table 1. Their values decrease with increase in illumination intensity. The Φ_B values obtained from the Norde method are in good agreement with the values obtained from I-V characteristics.

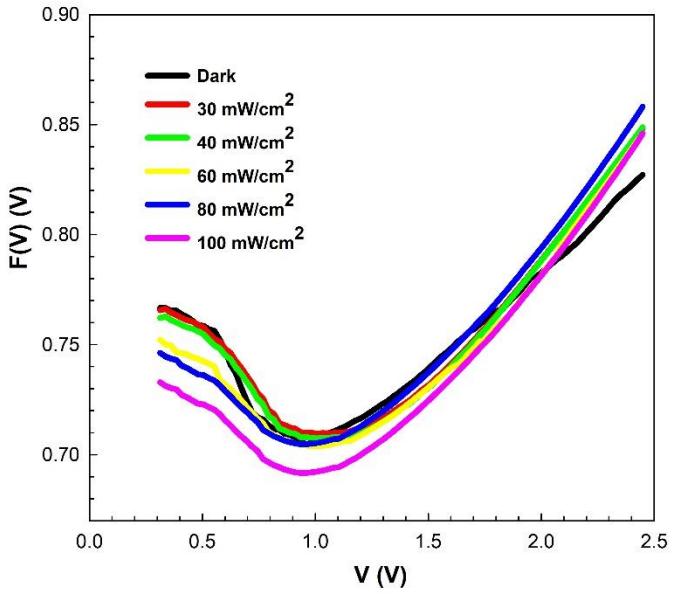

Fig. 3. F(V) versus V plots.

The magnitudes of shunt resistance (R_{sh}) and series resistance (R_s) and of the diode were determined using Ohm's law ($R_j=\partial V/\partial I$). The R_j-V plots at dark and under various illumination conditions are shown in Fig. 4. The calculated R_j value in high-reverse biases corresponds to the R_{sh}. The R_j value calculated at a sufficiently high-reverse bias voltage (at -2.5V) corresponds to the R_{sh}. The R_j value calculated at a sufficiently high-forward bias voltage (at +2.5V) corresponds to the R_s. The obtained R_{sh} and R_s values are given in Table 1. It is seen that the R_{sh} and R_s values decrease with increasing illumination intensity.

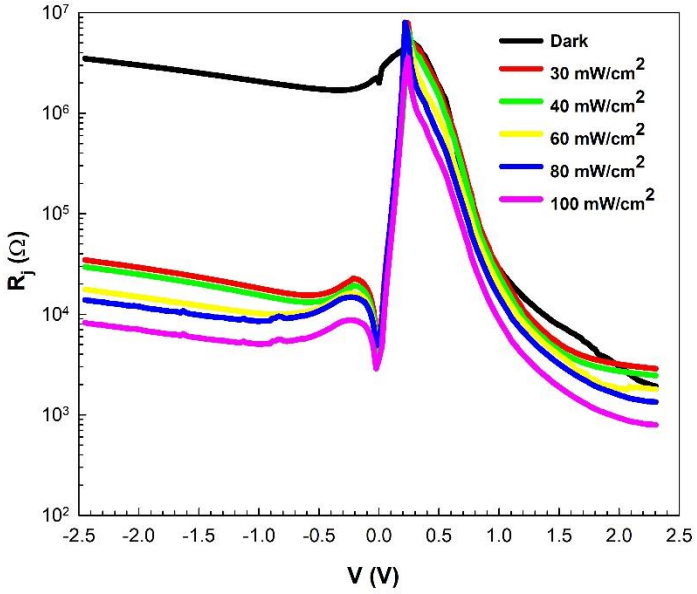

Fig. 4. The R_j-V plots.

The relation between the photocurrent (I_{ph}) and illumination intensity (P) is defined by the power law given as follows [31,32],

$$I_{ph} = AP^m \tag{6}$$

where m is an exponent extracted from the slope of Log(I_{ph}) versus Log(P) curve. A is a constant. Fig. 5 demonstrates the plot of Log(I_{ph})-Log(P) at bias voltage of -2.5 V. It is clear that this plot shows good linearity between the illumination and photocurrent. In other words, the MPS diode indicates a good photovoltaic behavior. The m value determined from the slope of the linear region was found to be 1.27. The m value ranging from 0.5 to 1 indicates the presence of the trap centers within the band gap. But, a higher value of m indicates a lower density of the unoccupied trap level [33-35].

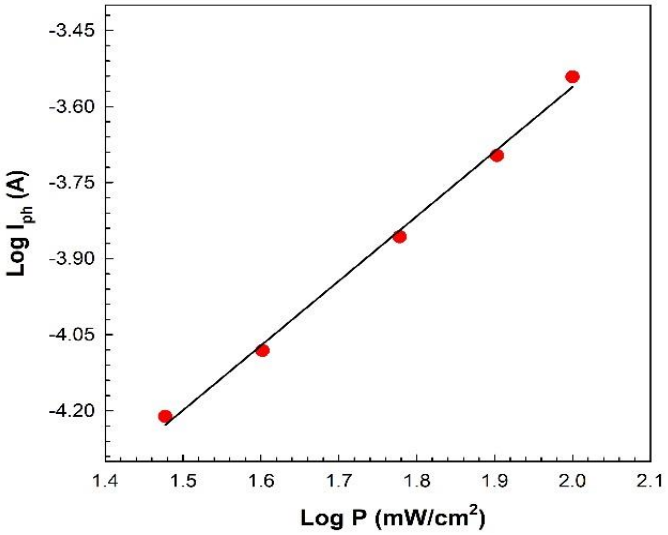

Fig. 5. Plot of Log(I_{ph}) versus Log(P).

The photocurrent (I_{ph}) to dark current (I_{dark}) ratio is defined by the photosensitivity (S_{ph}), and it is calculated as follows,

$$S_{ph} = \frac{I_{ph}}{I_{dark}} \tag{7}$$

Fig. 6 shows plot of S_{ph} versus incident illumination intensity (P) at -2.5 V. As seen in this figure, the photosensitivity increases with illumination intensity. The MPS diode exhibits high photosensitivity.

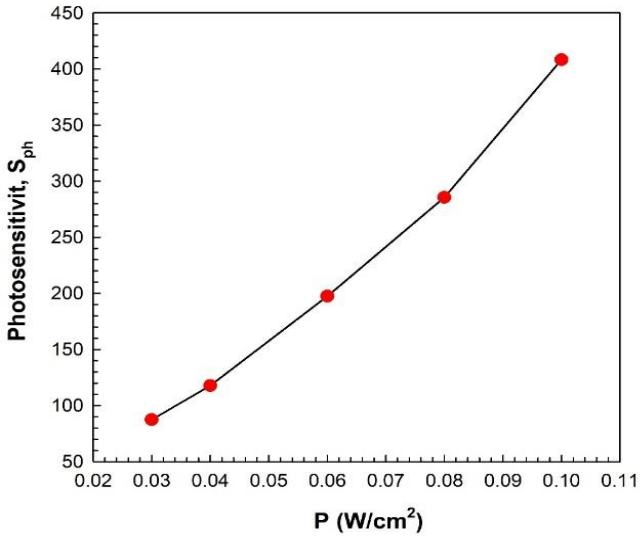

Fig. 6. Plot of S_{ph} versus P.

The responsivity (R) is a measure of the sensitivity to light and is calculated using the equation,

$$R = \frac{I_{ph}}{PA} \quad (8)$$

where P is the illumination power and A (=7.85x10^{-3}cm^2) is the diode area [35-39]. Similar results were also found in recently by some researchers [40-42]. Fig. 7 shows plot of responsivity versus P at the reverse voltage (-2.5 V). As seen in Fig. 7, the responsivity is increased with increasing incident illumination. This increase in the responsivity may be due to the excitation of electron-hole pairs from incident light.

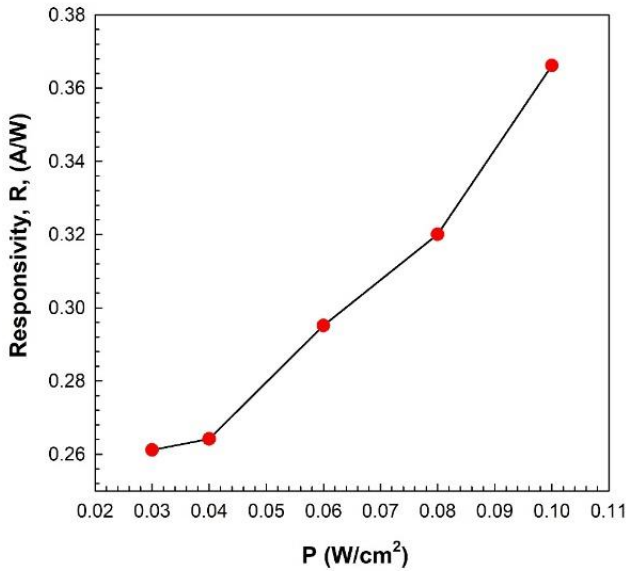

Fig. 7. Plot of responsivity versus P.

4. Conclusions

In this study, photoresponse and electrical properties of the fabricated Au/($CoFe_2O_4$-PVP)/n-Si (MPS) diode were investigated both in dark and under illumination density range of 30-100 mW.cm^{-2} by using the forward and reverse bias I-V measurements at room temperature. The diode electrical parameters including I_0, n, Φ_{B0}, and R_s were obtained from these data by using the standard TE theory and Norde method. All these electronic parameters were found strong function of illumination intensity and voltage and decrease with increasing illumination intensity level. Experimental results show a good linear correlation between Φ_{B0} and n as Φ_{B0}

(n)=4.72x10^{-2}n+0.5464 eV and hence the value of Φ_{B0} was found as 0.5936 ev for n=1 (ideal case). The illumination enhances the reverse current when compared to the forward current and so the diode has exhibited good photoconductivity or photovoltaic behavior. The results showed that the illumination has a significant effect on the current. In addition, the calculated sensitivity and responsivity of the MPS device showed a high photoresponse under various illumination intensities. As result, the prepared MPS diode may be used as photodiode, photodetector and photovoltaic cell in various optoelectronic applications.

Acknowledgements: *This study was supported by Gazi University Scientific Research Project. (Project Number: GU-BAP.05/2019-26).*

References

1. A. Tataroglu, S. Altındal, Y. Azizian-Kalandaragh, Physica B 576 (2020) 411733.
2. A. Gusain, R.M. Faria, P.B. Miranda, Front. Chem. 7 (2019) 61.
3. L.W. Lima, F. Aziza, F.F. Muhammad, A. Supangat, K. Sulaiman, Synthetic Metals 221 (2016) 169-175.
4. M. Tahir, M. Hassan Sayyad, F. Wahab, D. Nawaz Khan, F. Aziz, Physica B 415 (2013) 77-81.
5. F. Yakuphanoglu, Synthetic Metals 160 (2010) 1551-1555.
6. D. Wood, Optoelectronic Semiconductor Devices, Prentice Hall, New York, 1994.
7. J. Singh, Electronic and Optoelectronic Properties of Semiconductor Structures, Cambridge University Press, New York, 2003.
8. L.-Shu Wan, Z.-Kang Xu, Z.-Gang Wang, J. Polym. Sci. Part B: Polym. Phys. 44 (2006) 1490-1498.
9. S.A. Salman, A.A. Habeeb, A.A. Sallal, Indian J. Natural Sci. 9 (2019) 16651-16658.
10. H.M. Ragab, Physica B 406 (2011) 3759–3767.
11. S. Ningaraju, A.P. Gnana Prakash, H.B. Ravikumar, Solid State Ionics 320 (2018) 132-147.
12. B. Chaudhuri, B. Mondal, S.K. Ray, S.C. Sarkar, Colloids Surf. B: Biointerfaces 143 (2016) 71-80.
13. M. Teodorescu, M. Bercea, S. Morariu, Biotechnology Adv. 37 (2019) 109-131.
14. L.H. Sperling, Introduction to Physical Polymer Science, 4th Ed., Wiley, Hoboken, New Jersey, 2006.
15. J.R. Fried, Polymer Science and Technology, 3rd Ed., Prentice Hall, New Jersey, 2014.
16. W. Knoll, R.C. Advincula, Functional Polymer Films, Wiley-VCH Verlag, Weinheim, 2011.
17. A. Tataroglu, A. Buyukbas Ulusan, Ş. Altındal, Y. Azizian-Kalandaragh, J. Inorg. Organomet. Polymer Mater., https://doi.org/10.1007/s10904-020-01798-x.
18. S.M. Sze, Physics of Semiconductor Devices, 2nd Ed., Wiley, New York, 1981.
19. E.H. Rhoderick, R. H. Williams, Metal Semiconductor Contacts, 2nd Ed., Clarendon Press, Oxford, 1988.
20. F. Yakuphanoglu, A. Tataroğlu, A.A. Al-Ghamdi, R.K. Gupta, Y. Al-Turki, Z. Şerbetçi, S. Bin Omran, F. El-Tantawy, Solar Energy Mater. Sol. Cells 133 (2015) 69-75.
21. A. Tataroglu, Ş. Altındal, Y. Azizian-Kalandaragh, J. Mater. Sci.: Mater. Electron. 31 (2020) 11665-11672.
22. H. Dong, H. Zhu, Q. Meng, X. Gong, W. Hu, Chem. Soc. Rev. 41 (2012) 1754-1808.
23. H.H. Gullu, D.E. Yildiz, A. Kocyigit, M. Yıldırım, J. Alloys Compd. 849 (2020) 156628.

24. A.M. El-Mahalawy, M. Abd-El Salam, Appl. Phys. A 126 (2020) 393.
25. A. Büyükbaş Uluşan, A. Tataroğlu, Y. Azizian-Kalandaragh, Ş. Altındal, J. Mater. Sci.: Mater. Electron. 29 (2018) 159-170.
26. A. Kumar, A. Kumar, K.K. Sharma, Subhash Chand, Superlattices Microst. 128 (2019) 373-381.
27. F.Z. Pur, A. Tataroglu, Phys. Scripta 86 (2012) 035802.
28. A. Tataroglu, S. Altındal, M.M. Bulbul, Nucl. Instrum. Methods. Phys. Res. A 568 (2006) 863-868.
29. S. Karatas, H.M. El-Nasser, A.A. Al-Ghamdi, F. Yakuphanoglu, Silicon 10 (2018) 651-658.
30. H. Norde, J. Appl. Phys. 50 (1979) 5052-5054.
31. A. Rose, Concepts in Photoconductivity and Allied Problems, Interscience, New York, 1963.
32. R. H. Bube, Photoelectronic Properties of Semiconductors, Cambridge University Press, Cambridge, 1992.
33. F. Yakuphanoglu, Composites Part B 92 (2016) 151e159
34. A. Mekki, R.O. Ocaya, A. Dere, Ahmed A. Al-Ghamdi, K. Harrabi, F. Yakuphanoglu, Synth. Metals 213 (2016) 47-56.
35. O. Çiçek, H. Uslu Tecimer, S.O. Tan, H. Tecimer, I. Orak, S. Altındal, Comp. Part B 113 (2017) 14-23.
36. K. Ozel, A. Yildiz, Sens. Actuators A 315 (2020) 112351
37. E. Cuculescu, I. Evtodiev, E. Arama, M. Caraman, Moldavian J. Phys. Sci. 7 (2008) 55-60.
38. E. Wu, D. Wu, C. Jia, Y. Wang, H. Yuan, L. Zeng, T. Xu, Z. Shi, Y. Tian, X. Li, ACS Photonics 6 (2019) 565-572.
39. H.S. Wasly, M.S. Abd El-sadek, G. Karczewski, I.S. Yahia, J. Mater. Sci.: Mater. Electron. 30 (2019) 4936-4942.
40. G. Imer, E. Kaya, A. Dere, A. G. Al-Sehemi, A. A. Al-Ghamdi, A. Karabulut, F. Yakuphanoglu, J. Mater. Sci.: Mater. Electron 31 (2020) 14665-14673.
41. A. Dere, B. Coskun, A. Tataroglu, A. G. Al-Sehemid, A. Al-Ghamdig, M.A. Hind. Alateeqh, R. Qindeelh, W.A. Farooqh, F. Yakuphanoğlu, Physica B 545 (2018) 86-93.
42. S. Demirezen, H.G. Çetinkaya, M. Karac, F. Yakuphanoglu, Ş. Altındal, Sens. Actuator A 317 (2021) 112449.

Figures

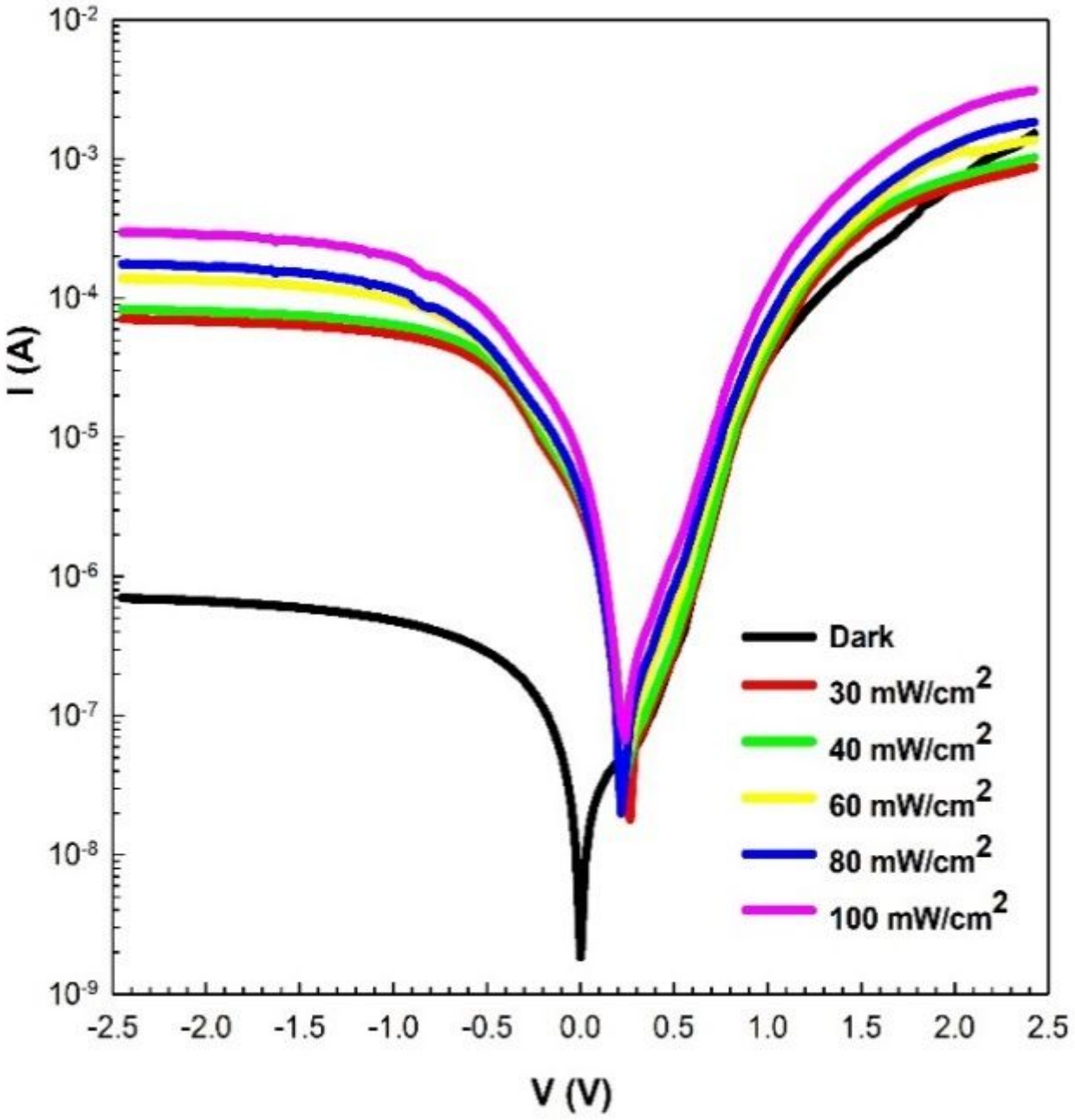

Figure 1

Semi-logarithmic I-V characteristics of the MPS diode.

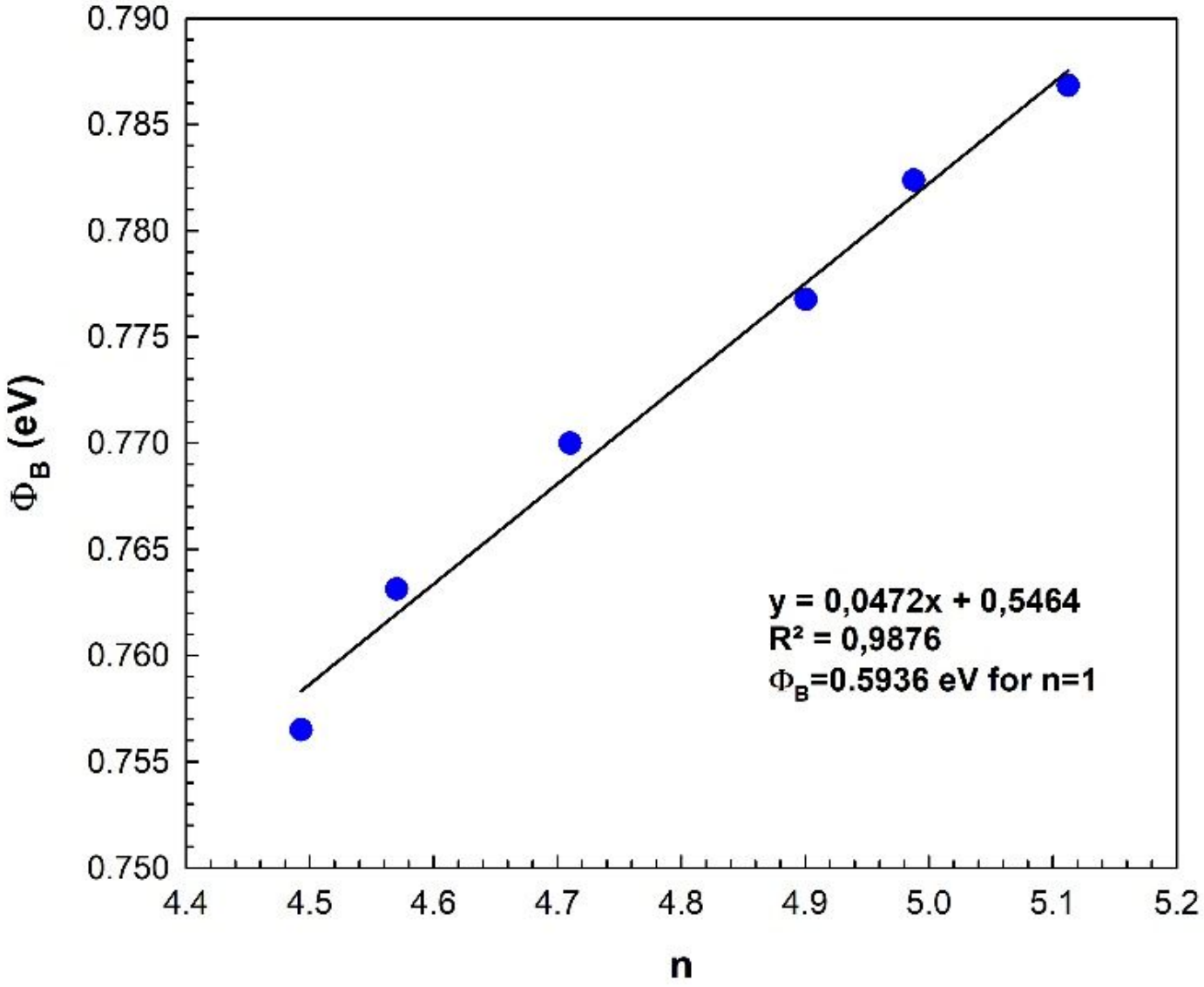

Figure 2

The plot of ΦB0-n characteristics.

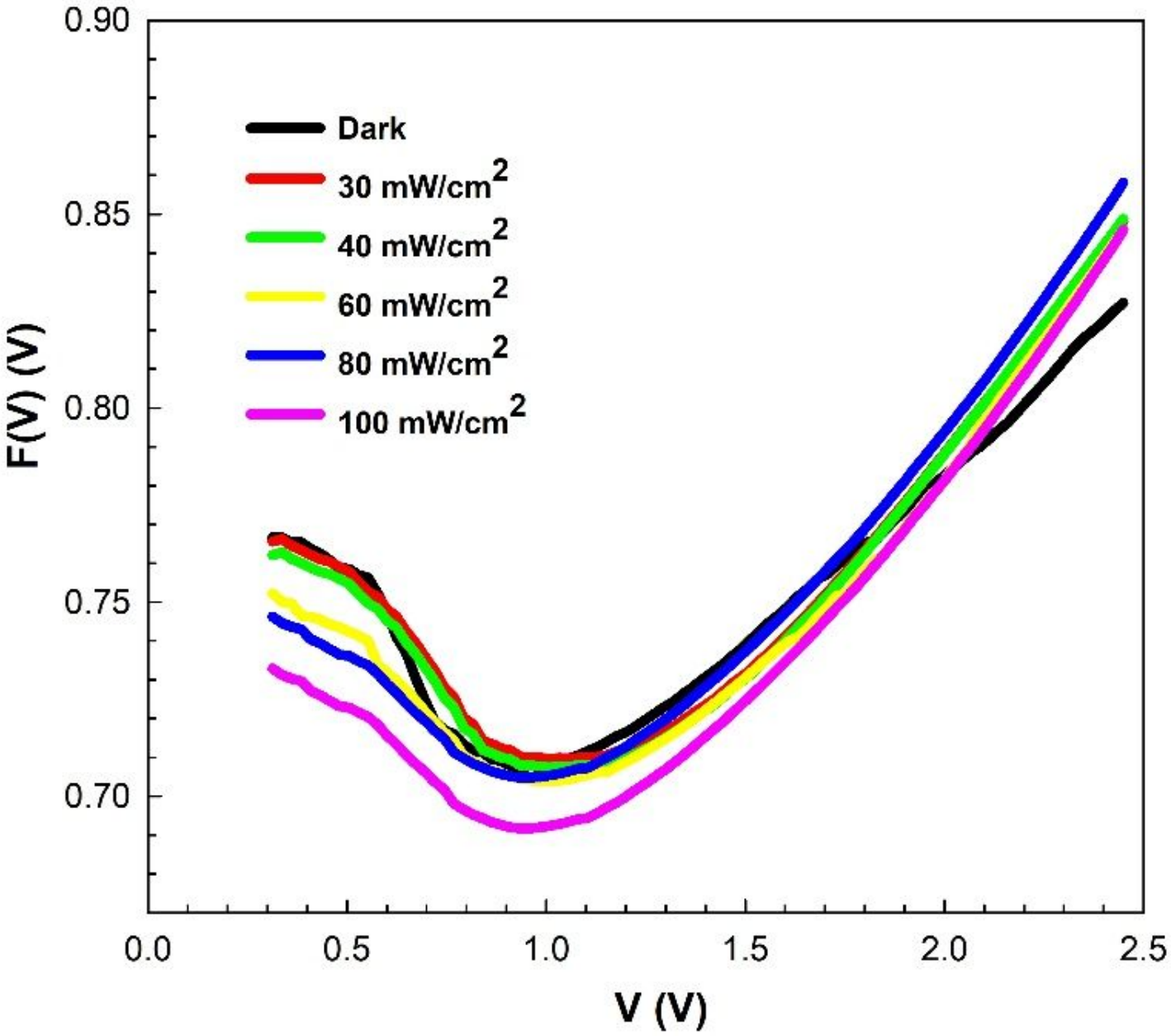

Figure 3

F(V) versus V plots.

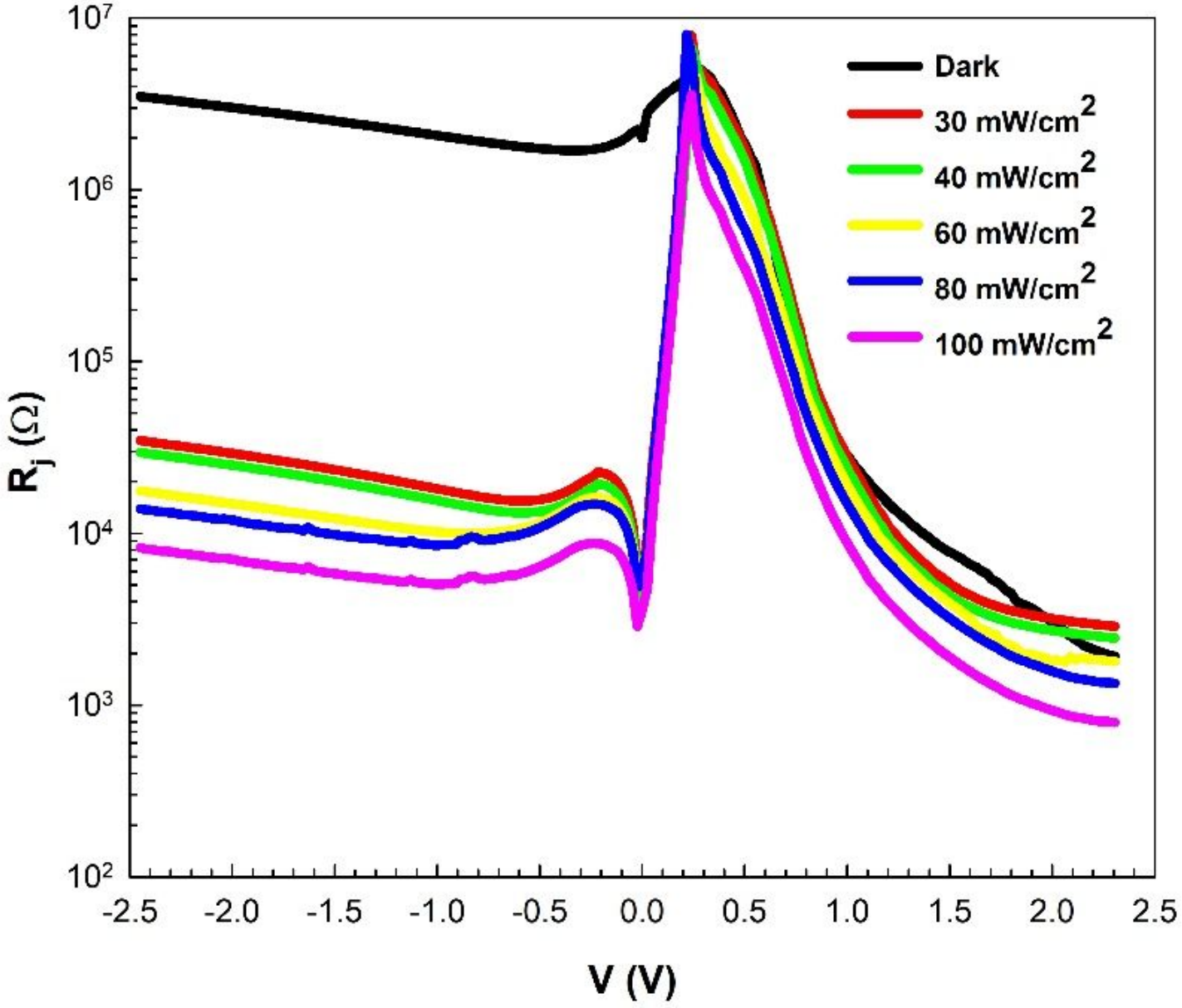

Figure 4

The Rj-V plots.

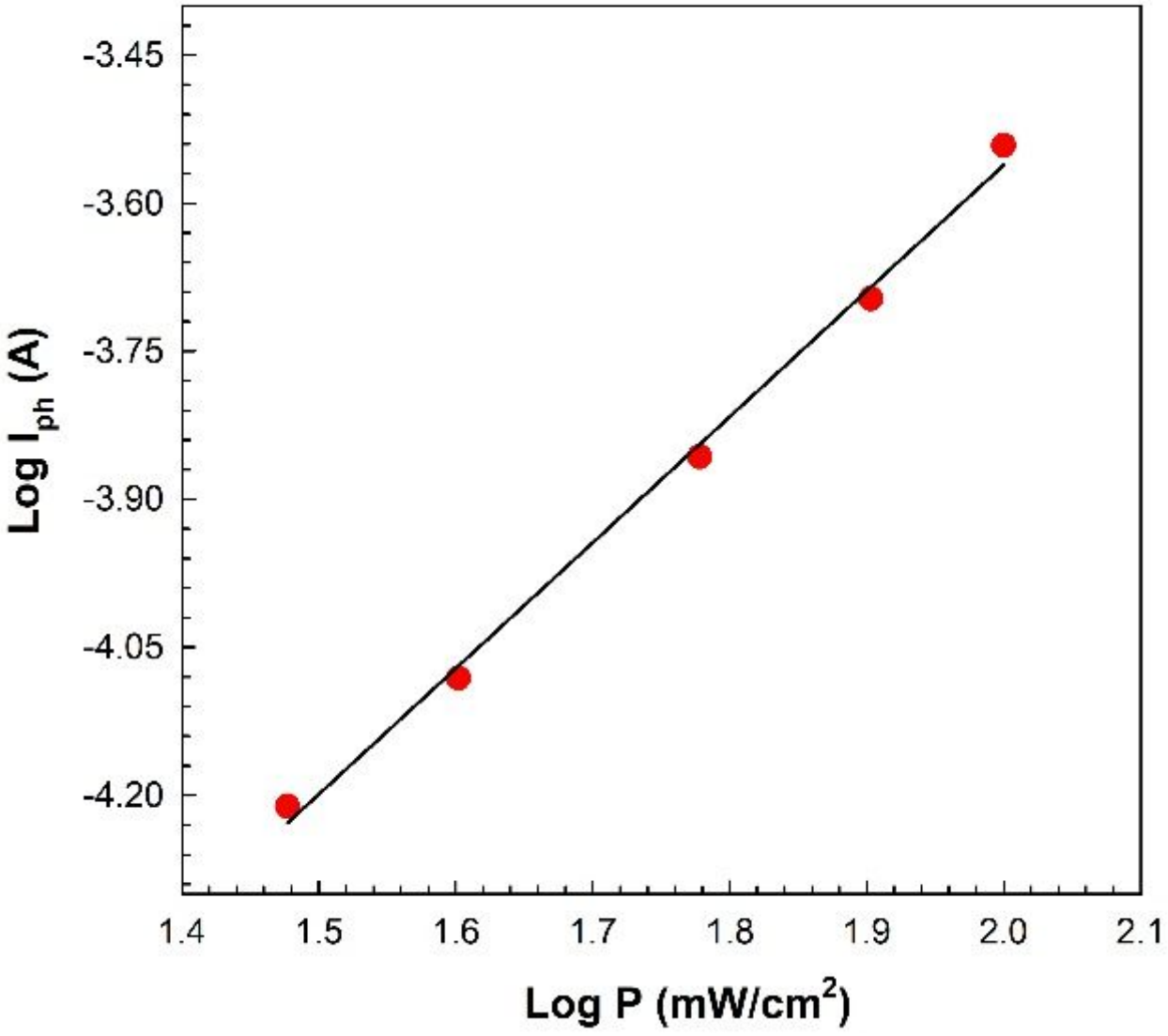

Figure 5

Plot of Log(Iph) versus Log(P).

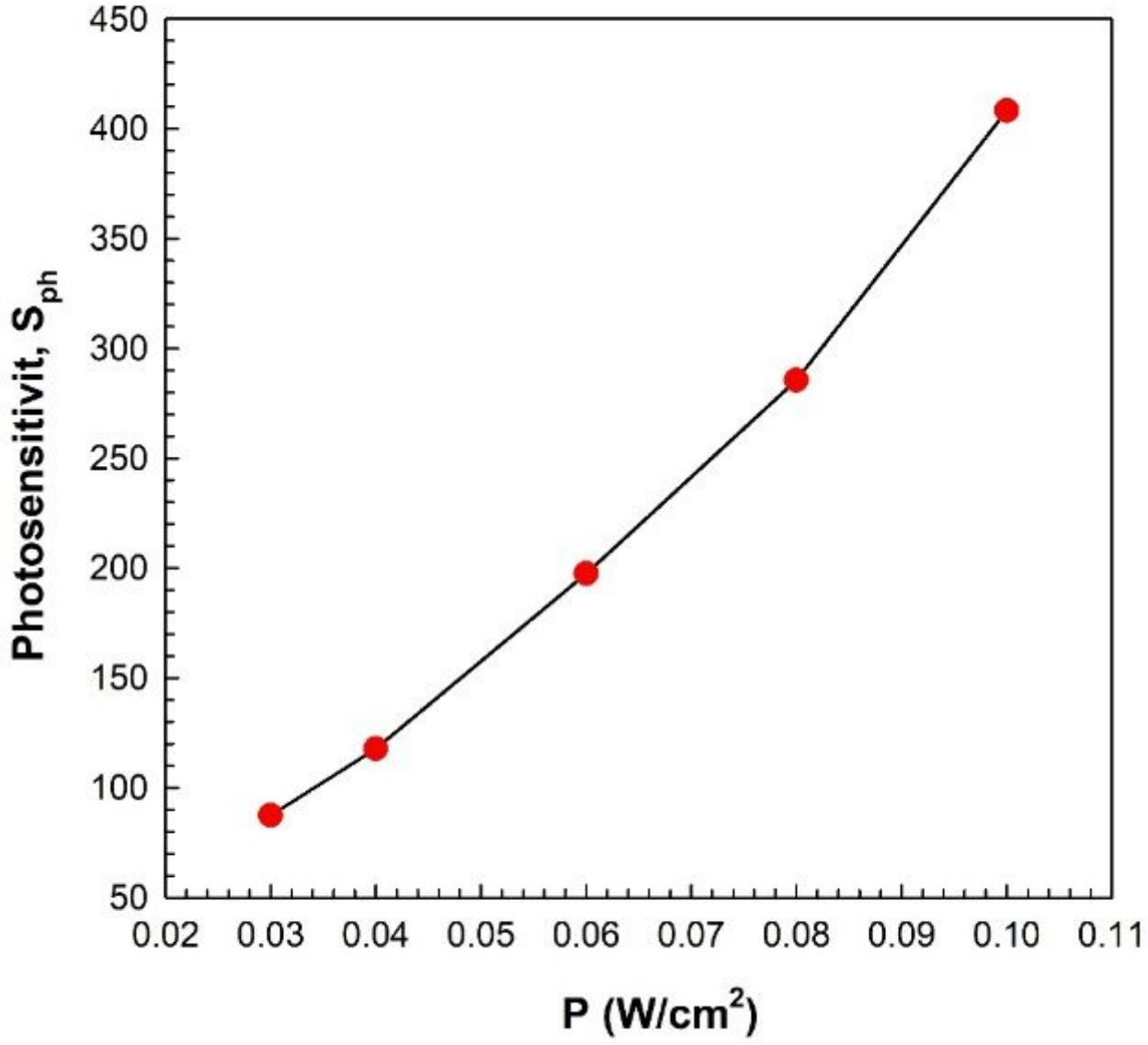

Figure 6

Plot of Sph versus P.

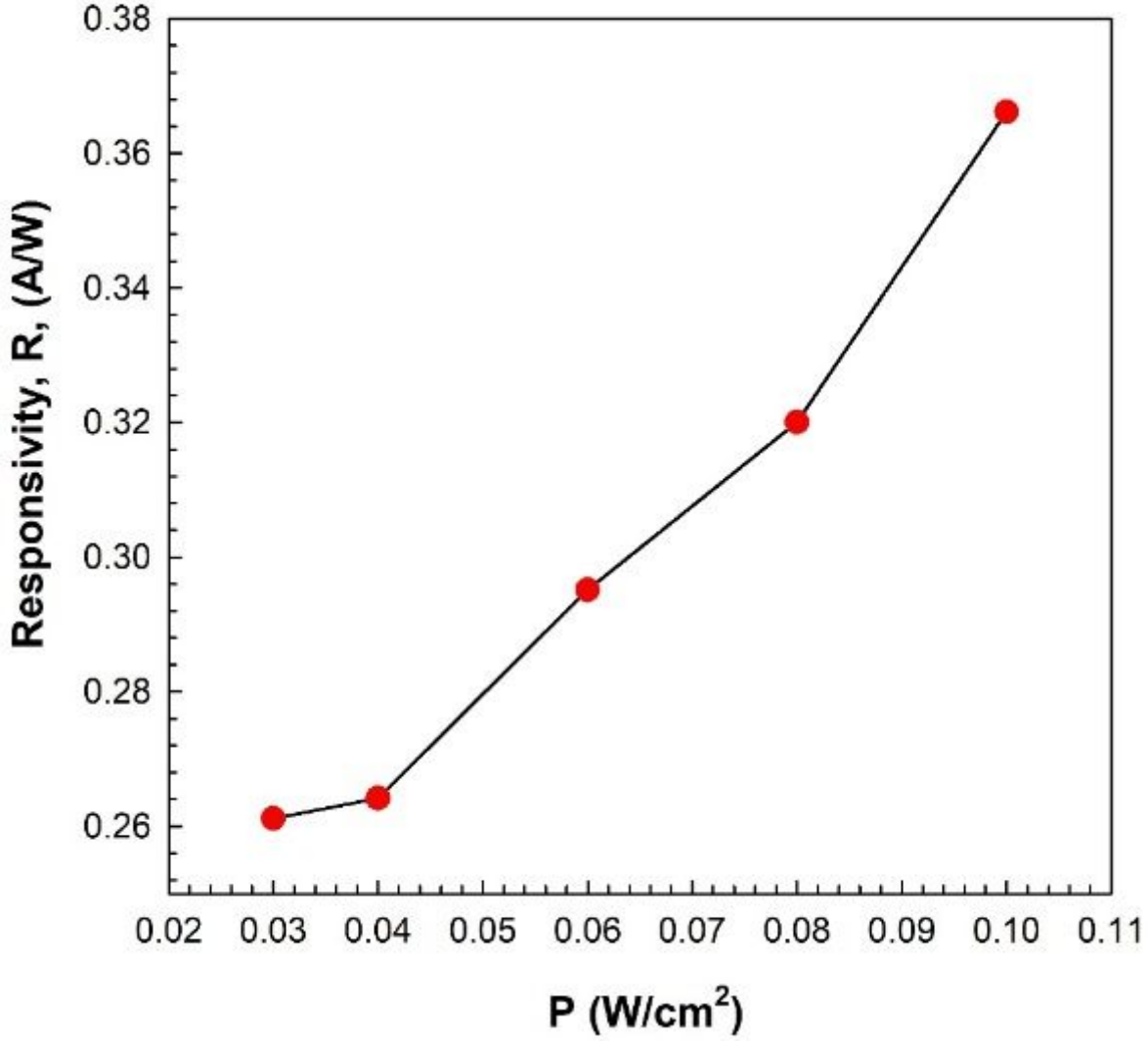

Figure 7

Plot of responsivity versus P.